1

Effect of Severe Plastic Deformation on the Properties and Structural Developments of High Purity Al and Al-Cu-Mg-Zr Aluminium Alloy

Tibor Kvačkaj[1], Jana Bidulská[1], Robert Kočiško[1] and Róbert Bidulský[2]
[1]*Technical University of Kosice, Faculty of Metallurgy, Department of Metals Forming*
[2]*Politecnico di Torino – Sede di Alessandria*
[1]*Slovakia*
[2]*Italy*

1. Introduction

Demands of industry producers are to find new forms and facilities for appropriate properties of structural parts suitable for different miscellaneous structural applications in the civil, automotive and aircraft industries. With respect to these facts, aluminium alloys find a wide variety of uses due to their remarkable combination of characteristics such as the low density, the high corrosion resistance, high strength, easy workability and high electrical and heat conductivity.

The traditional process is to obtain the improvement in the mechanical properties of aluminium alloys through the precipitation of a finely dispersed second phase in the matrix. This is accomplished by a solution treatment of the material at a high temperature, followed by quenching. The second phase is then precipitated at room or elevated temperatures. For aluminium alloys this procedure is usually referred to as age hardening and it is also known as precipitation hardening (Michna et al., 2007); (Mondolfo, 1976). Conventional forming methods are ineffective in the achieving of favourable properties area of produced parts, adequate to structural properties; moreover through them only limited levels of structural and strength-plastic characteristics can be obtained. The solution may be non-conventional forming methods (Kvačkaj et al., 2005), (Kvačkaj et al., 2004), (Kvačkaj et al., 2010 a) as well as Severe Plastic Deformation (SPD), such as more preferable are equal channel angular pressing - ECAP, (Valiev & Langdon, 2006), (Valiev et al., 2000) to obtain results structured at the nm level. A combination of high strength and ductility of ultrafine polycrystalline metals, prepared by SPD, is unique and it indeed represents interesting cases from the point of view of mechanical properties (Chuvil'deev et al, 2008); (Zehetbauer et al., 2006); (Han et al., 2005) ;(Ovid'ko, 2005); (Meyers et al., 2006); (Kopylov & Chuvil'deev, 2006); (Zehetbauer & Estrin, 2009). In the past decade, the research focused on to strengthen Al alloys without any ageing treatment, via SPD (Kvačkaj et al., 2010 b).

The finite element method (FEM) is a proven and reliable technique for analyzing various forming processes (Kvačkaj et al., 2007); (Kočiško et al., 2009); (Li et al., 2004); (Leo et al., 2007); (Cerri et al., 2009), (Figueiredo et al., 2006); (Mahallawy et al., 2010); (Yoon & Kim, 2008), in order to analyze the global and local deformation response of the workpiece with

nonlinear conditions of boundary, loading and material properties, to compare the effects of various parameters, and to search for optimum process conditions for a given material (Kim, 2001).

The unique mechanical properties of the ECAPed material are directly affected by plastic deformation. Hence, the understanding the development of strain during processing has a key role for a successful ECAP process. It is well known that the main factors affecting the corner gap formation during ECAP are materials strain hardening and friction. Thus, character of the strained condition and uniformity of plastic flow during ECAP is very sensitive to friction coefficient (Balasundar & Raghu, 2010); (Zhernakov et al., 2001); (Medeiros et al., 2008).

In order to understand various processes like as the workpiece (billet), die design, the friction conditions, etc.; it is essential to combine experimental research with a theoretical analysis of inhomogeneous deformation behaviour in the workpiece during the process.

In addition to the aforementioned properties, the most important factor affecting the mathematical simulation of material is the stress-strain curve (stress-strain curve influences the calculation precision). These data can be derived either from database program or from experimental achieved stress-strain curve. Experimental stress-strain curve can easily be determined by laboratory tests of formability. The most frequently used formability tests are torsion and tension (Pernis et al., 2009); (Kováčová et al., 2010).

Structure investigations by TEM analysis will be useful key to identifications and confirmations the various theories about the material behaviour during the ECAP processing (Dutkiewicz et al., 2009); (Dobatkin et al., 2006); (Lityńska-Dobrzyńska et al., 2010); (Maziarz et al., 2010); (Alexandrov et al., 2005).

The present chapter book focused on the effect of Severe Plastic Deformation on the properties and structural developments of high purity aluminium and Al-Cu-Mg-Zr aluminium alloy.

Former part deals with the high purity aluminium (99,999 % Al) processed by six ECAP passes in room temperature. Influence of strain level, strength, microhardness, plasticity and diameter of grain size in dependence on ECAP passes were investigated. FEM analysis with respect to influence friction coefficient (f=0,01-0,3) and characteristic of deformed materials as such materials with linear and nonlinear strengthening on homogeneity of effective deformations during sample cross section were observed.

Latter part deals with the tensile properties as function of the processing conditions of the Al-Cu-Mg-Zr aluminium alloy. Based on the results above, the tensile properties, hardness and structure development of the Al-Cu-Mg-Zr aluminium alloy along with the numerical simulation are discussed.

2. Experimental conditions

2.1 Experimental conditions for investigation of high purity Al (99,999%Al)

Experimental material was prepared by zonal refining. Structure after producing was heterogeneous with average grain size d_g ~ 650 μm. Mechanical properties before ECAP processing are given in Table 1.

The ECAP process was carried out at room temperature by route C (sample rotation around axis about 180° after each pass) in an ECAP die with channels angle Φ = 90°. The rod-shaped samples (d_0 = 10 mm, l_0 = 80 mm) were extruded twelve ECAP passages at rate of 1 mm·s^{-1}. The deformation forces during ECAP sample processing was measured using tensometric measurement with LabVIEW apparatus.

0,2%YS [MPa]	UTS [MPa]	El. [%]	HV10[-]
36	52	27	24,2

Table 1. Initial mechanical properties of high purity aluminium (99,999 %)

The static tensile test on the short specimens d_0 x l_0 = 5 x 10 mm was performed. Tensile test was done after every second ECAP pass on ZWICK 1387 equipment by standard conditions EN 10002-1. Subsequently, characteristics of the strength (yield strength: YS; ultimate tensile strength: UTS) and elongation (El.) were determined.
The microhardness test was done on polished surface in longitudinal direction of sample after every second ECAP pass on LECO LM 700 AT equipment.
Transmission electron microscopy (TEM) analysis with electron diffraction in longitudinal direction of sample was done on thin foils on Philips CM 20 microscope. The thin foils were prepared using a solution of 5 % HF at a temperature -25 °C and the time 20 - 30 s.
Material flow in ECAP die was investigated. The samples were longitudinal cutting by wire cutter. Cutting surfaces were processing by metallographic grinding and polishing. Polishing surfaces were mechanically marked by square net as is given in Fig. 1. The size of one element was 1 x 1 mm. The samples after marking were again to join together and put in to ECAP unit. Orientation of sample cutting plane was identical with the plane lying in horizontal and vertical cannel axes. One pass in ECAP unit at rate 1 mm·s^{-1} was performed.

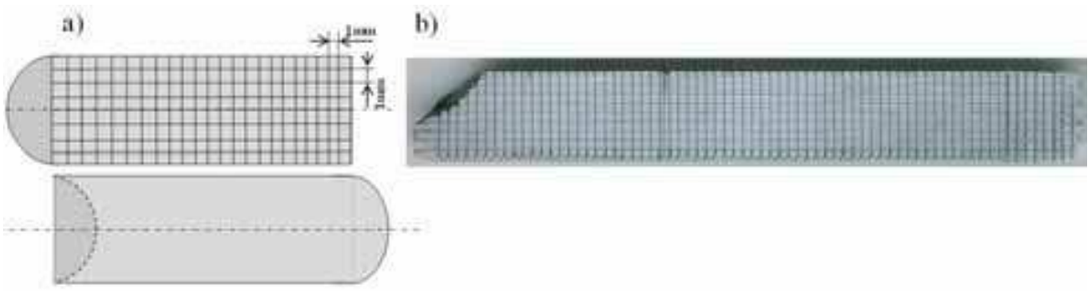

Fig. 1. Sample preparation before ECAP a) scheme of square net implementation on polishing surfaces, b) real Al sample with square net

Simulation of ECAP pass was carried out using the finite element method (FEM) in software DEFORM 2D as considering plane strain conditions (Deform Manual, 2003). Die geometries were directly designed in the software Deform 2D. The parameters were: circle canal of die with diameter, d_0 =10 mm, length, L=100 mm, die with channels angle, Φ = 90°, outer radius, R = 5 mm and inner radius, r = 0 mm. The workpiece dimensions were: diameter, d_0 =10 mm and length, l_0 = 80 mm. The processing rate was constant, v = 1 mm·s^{-1}. Friction was superposed to follow Coulomb's law with friction coefficient f = 0,12. The processing temperature was 20 °C. The theory at the base of FEM implies that at first, the problem has to be divided into little sub problems that are easily to be formulated. There over, they must all be carefully combined and then solved. The manner in which a problem is divided constituents the so called meshing process. Mesh density refers to the size of elements that will be generated within an object boundary. The mesh density is primarily based on the specified total number of elements. Mesh density according to (Kobayashi & Altan, 1989); (Deform Manual, 2003) is defined by the number of nodes per unit length, generally along the edge of the object. The mesh density values specify a mesh density ratio between two regions in the object. Even though the material properties are same, meshing is the most

important factor which will influence the finite element simulation results. The mesh size specifically influences the corner gap formation.
A higher mesh density offers increased accuracy and resolution of geometry, on the other the time required for the computer to solve the problem increases as number of nodes increases. An optimal meshing density has to be chosen according to the geometry and size of object according in (Kvačkaj et al., 2007); (Kočiško et al., 2009); (Li et al., 2004) specimen with diameter d_0 = 10 mm has been decided using 20 elements along the width. Hence, the specimen with diameter d_0 = 10 mm and length l_0 = 80 mm was meshed with 3000 elements, that's to say 28 elements on the specimen diameter, as shown in Fig. 2.

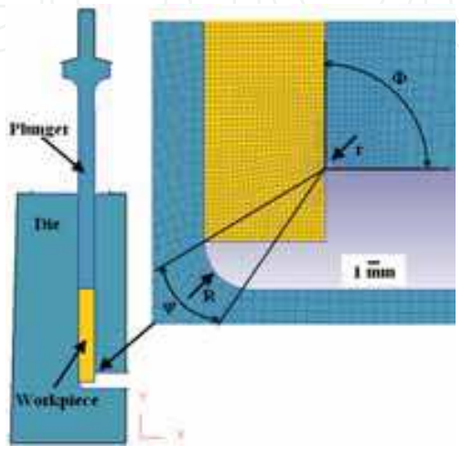

Fig. 2. FEM simulation scheme of ECAP

The finer meshes were built close to the surface in order to better match the geometry of the process, for example in channel areas. Authors (Semiatin et al., 2000) showed that the influence of channel angles of ECAP equipment was influencing the development of effective strain. Thus the highest effective strain is achieved if the angle between channels is 90°.
The tools of ECAP equipment (the die and plunger) were assumed to be elastic materials and they were assigned of tool steel material characteristic, them being much higher than those of deformed material. The specimen was assumed as elasto-plastic object with their material characteristics characterized by stress-strain curve Fig. 3.

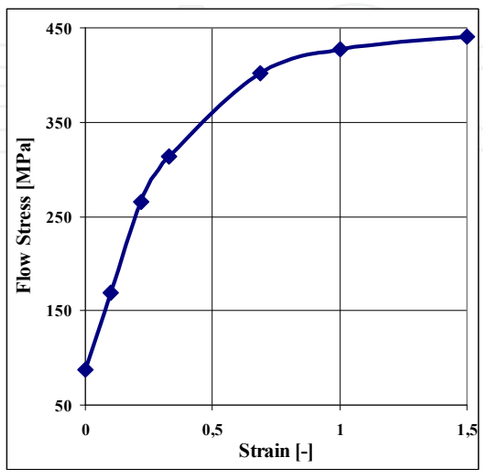

Fig. 3. Stress-strain curve of Al material

2.2 Experimental conditions for investigation of Al-Cu-Mg-Zr aluminium alloy

The material used in this experiment was Al-Cu-Mg-Zr aluminium alloy. The chemical composition is presented in Table 2.

Al	Cu	Mg	Mn	Si	Fe	Zr	Ti
balance	4,32	0,49	0,77	0,68	0,23	0,12	0,03

Table 2. Chemical compositions (wt. %) of investigated aluminium alloys

Hot rolling was carried out by rolling-mill DUO 210 at temperature of 460 °C (as-rolled state). Solution annealing after rolling was performed at temperature of 520 °C (holding time 9 000 s) and cooled to the room temperature by water quenching (quenched state). The quenched specimens (d_0 = 10 mm, l_0 = 70 mm) were subjected to deformation in an ECAP die with channels angle $\Phi = 90°$ at rate of 1 mm·s^{-1} (ECAPed state). The ECAP was realized by hydraulic equipment at room temperature. After one ECAP pass, the specimens were processed to artificial ageing at 100 °C for 720 000 s (ECAPed + aged state).

Tensile specimens were taken after each processing treatments. The tensile testing was done on a FP 100/1 machine with 0,15 mm·min^{-1} cross-head speed (strain rate of 2,5·10^{-4} s^{-1}). Static tensile test on the short specimens d_0 x l_0 = 5 x 10 mm was performed. Subsequently, characteristics of the strength (YS; UTS), El. and Re. were determined.

For optical microscopy, samples were individually mounted, mechanically polished and finally etched at room temperature using a mixture of 2 % HF, 3 % HCl, 5 % HNO_3 and 90 % H_2O (Keller's Reagent).

TEM analysis was performed on thin foils. The foils for TEM were prepared using a solution of 25 % HNO_3 and 75 % CH_3OH at a temperature -30 °C. TEM was conducted at an accelerating voltage of 200 kV.

Additionally, a fractographic study of the fracture surface of the materials after a conventional tensile strength test was carried out using SEM JEOL 7000F.

The numerical simulation of ECAP process was similar as is described in capture 2.1. Only sample length l_0 = 60 mm was changed. The specimen was assumed as elasto-plastic object with their material characteristics characterized by stress-strain curve (Table 3), Young's modulus and thermal properties. Certainly, the simulation conditions of investigated materials were considered so that the bounds of the deformation strain, strain rate and deformation temperature can't lead to loss of accuracy.

Strain [-]	0	0,1	0,2	0,3	1
Database data / stress [MPa]	0	200	233	250	312
Experimental data / stress [MPa]	0	68	144	174	324

Table 3. Stress-strain data of Al-Cu-Mg-Zr aluminium alloy for both conditions

Materials characteristics for both conditions are presented in Table 4.

Hence, mathematical simulations of ECAP process of Al-Cu-Mg-Zr aluminium alloy were realized on the basis of two approaches for stress-strain curve selection: from DEFORM material database and from experimental results. The DEFORM material database contains flow stress data for Al-Cu-Mg-Zr aluminium alloy (Table 3). The flow stress data provided by the material database has a limited range in terms of temperature range and effective strain.

Workpiece		Database	Experimental
Plastic		Flow stress (Table 2)	
Elastic	Young's modulus [MPa]	68900	70000
	Poisson's ratio [-]	0,33	0,33
	thermal expansion [K^{-1}]	$2{,}2 \cdot 10^{-5}$	$2{,}2 \cdot 10^{-5}$
Thermal	thermal conductivity [kW/m·K]	180,2	180,2
	heat capacity [$kJ \cdot kg^{-1} \cdot K^{-1}$]	2,433	2,433
Damage model (Fracture data)		Cockcroft-Latham	

Table 4. Materials characteristics for both investigated specimens

3. Results and discussion

3.1 Experimental results and discussion for high purity Al (99,999%Al)

3.1.1 FEM investigation

The deformed net after 1st ECAP pass is shown in Fig. 4a. Deformed net on sample surfaces was scanning and computer cover by new net for better visualisation as is given on Fig. 4b. Numerical simulations of net deformation in software DEFORM 2D are shown in Fig. 4c.

The intensity of plastic deformation is depended on angle of shearing strain γ. With increased of shearing strain angle is increasing also intensity of plastic deformation. The net deformation of sample is pointing out localization of biggest plastic deformation to top sample part which correspond with inner radius (r) of ECAP channel. The value of this shearing strain angle is γ = 60°. This value is observing up to 2/3 of sample cross section. Started from 2/3 of top to bottom sample part shearing strain angle is rapid decreasing up to level γ = 8°. Reported by authors (Beyerlein et al., 2004); (Stoica et al., 2005) this low level is characterizing by straining way in deformation zone which is more bending as plastic flowing. Mutual comparison of shearing strain angles γ obtained from experiment and numerical simulation reference to high conformity of results. Some difference was observed only in 1/5 bottom sample part where preferable deformation is bending.

The ECAP channel filling by processing material has influence on distribution of effective plastic deformation, which depends on: contact friction, stress – strain (σ-ε) curves characterizing deformed material and geometrical definition of ECAP die (Li et al., 2004). For numerical simulation of 1st ECAP pass geometrical definition of channels was as follow: Φ = 90°, R = 0 mm and r = 0 mm. The influence of friction coefficient in interval f = 0,01 – 0,25 on channels filling was simulated as is shown in Fig.5.

If geometrical definition of channels (Fig. 6) was describe by formula (1) (Oh et al., 2003) that linear graphical dependence shown in Fig. 7 was obtained.

$$\lambda = d_h \cdot \left(1 + \frac{d_h}{d_v}\right) \tag{1}$$

where: λ [-] – index for the outer corner
d_h [mm] – distance between die corner and horizontal contact point of die and workpiece
d_v [mm] – distance between die corner and vertical contact point of die and workpiece

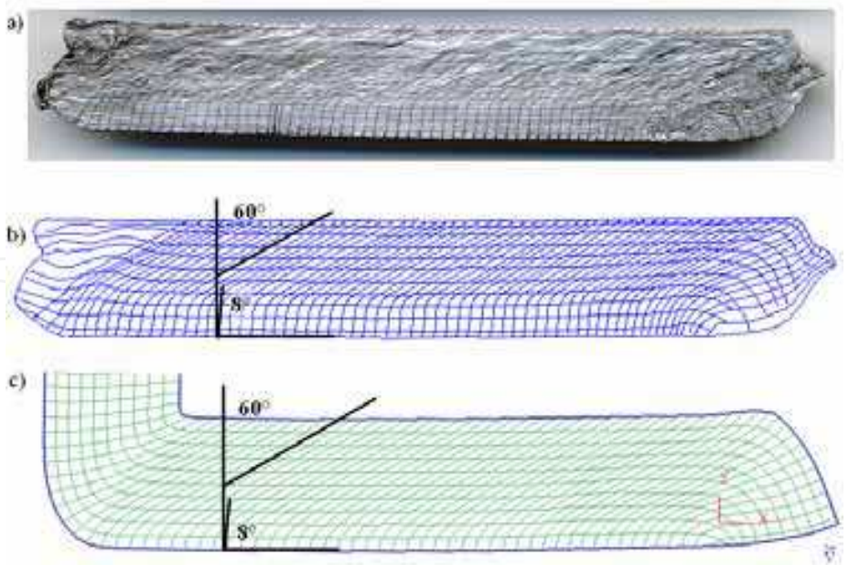

Fig. 4. Deformed net after 1st ECAP pass a) Deformed net on real sample, b) Visualisation deformed net after scanning and computer redrawing with marking of angle of shearing strain γ, c) Deformed net after numerical simulation in DEFORM 2D

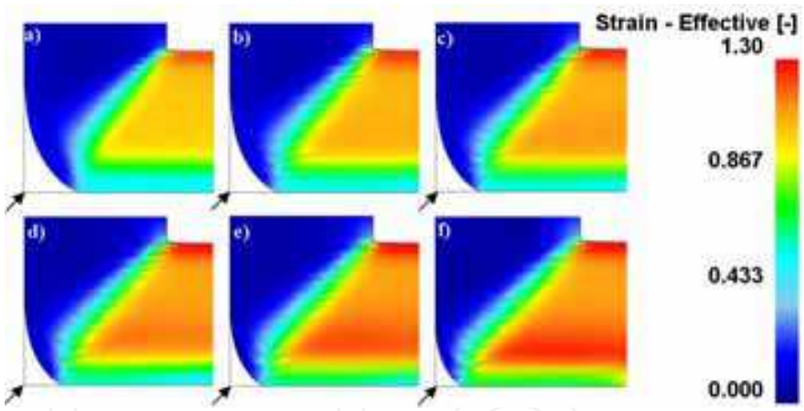

Fig. 5. ECAP channels filling in dependence on friction coefficient: a) f = 0,01; b) f = 0,12; c) f = 0,18; d) f = 0,25; d) f = 0,3 a e) f = 0,35

From graph is resulting that better channels filling by material were obtained when friction coefficient was increased. The numerical simulations confirm biggest localization of effective strain heterogeneity to bottom side of sample as is shown in Fig. 8.

The influence of σ-ε curves characterizing deformed material on channels filling was numerical simulated for σ-ε curves with linear (Fig. 9) and nonlinear (Fig. 10) strengthening. The measurement of lengths d_h and d_v for both type of σ-ε curves are given in Fig. 11, Fig. 12 and dependence of shape index of outer corner on angle of curves inclination is given in Fig. 13. From graphical dependences is resulting negligible influence of σ-ε strengthening type curves (linear and nonlinear strengthening) on channels filling for curve types 1-5. If strengthening curves are approaching to ideal rigid – plastic form with minimal strengthening (types 6-7) so differences in channel filling are observing.

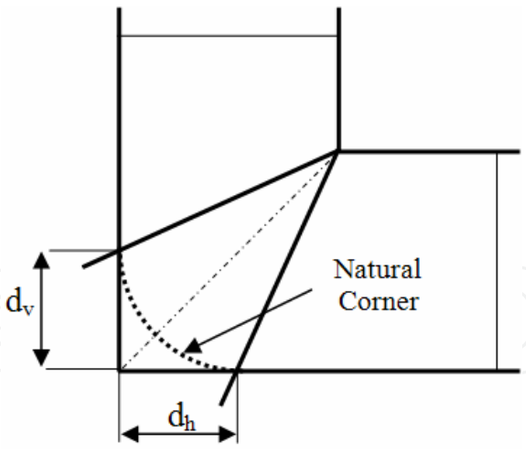

Fig. 6. Geometrical definition of channels

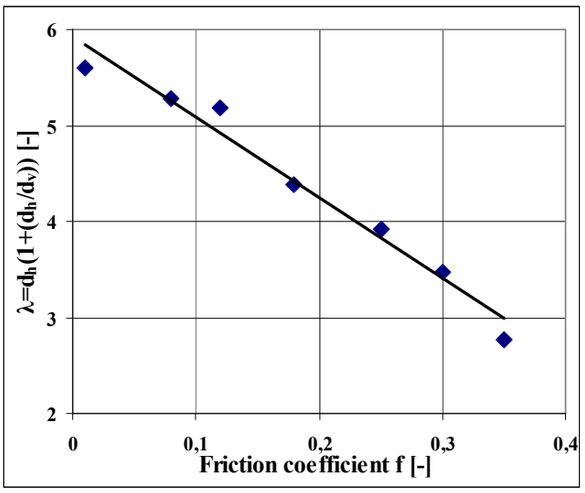

Fig. 7. Dependence of index of outer corner shape on friction coefficient

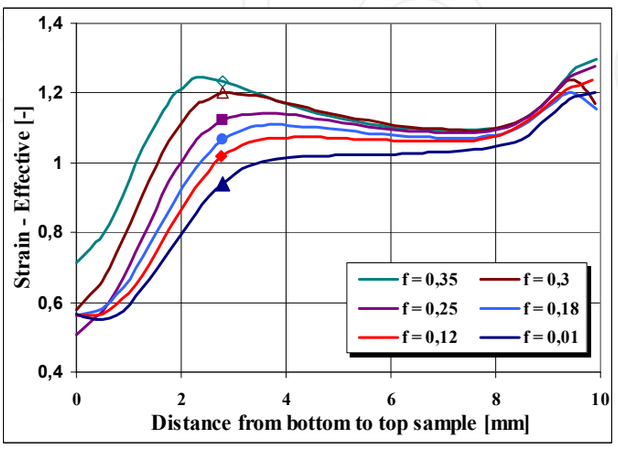

Fig. 8. Distribution of effective strain φ_{ef} in cross section sample on friction coefficient

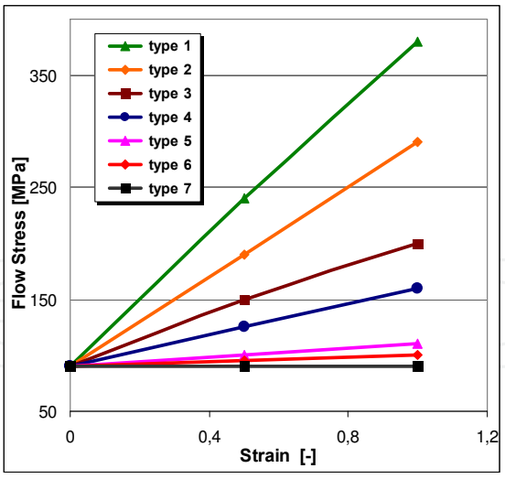

Fig. 9. The σ - ε curves with linear strengthening

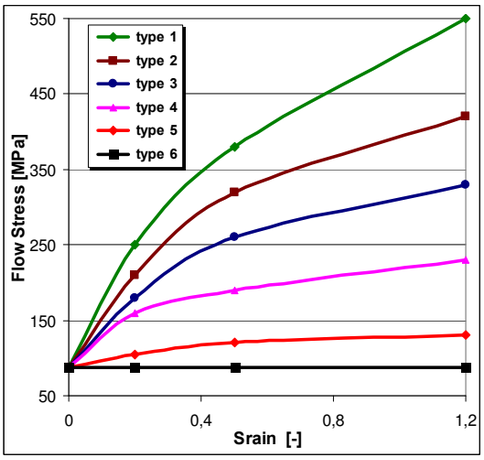

Fig. 10. The σ - ε curves with nonlinear strengthening

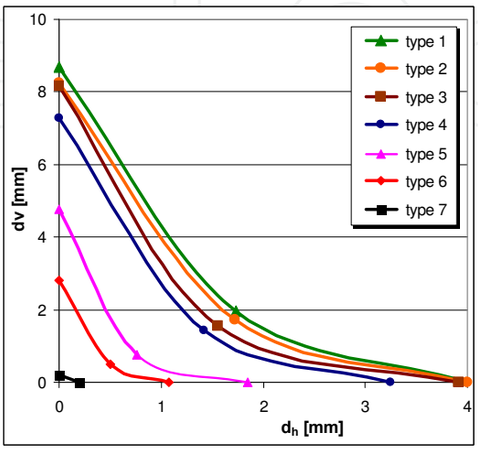

Fig. 11. Effect of σ - ε curves with linear strengthening on the channel outer filling

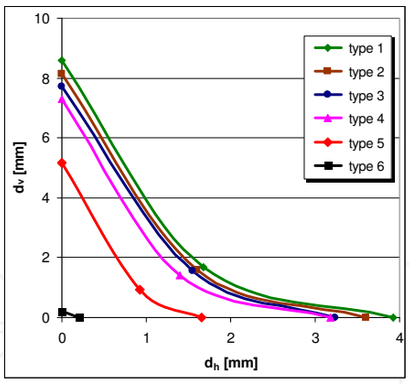

Fig. 12. Effect of σ - ε curves with nonlinear strengthening on the channel outer filling

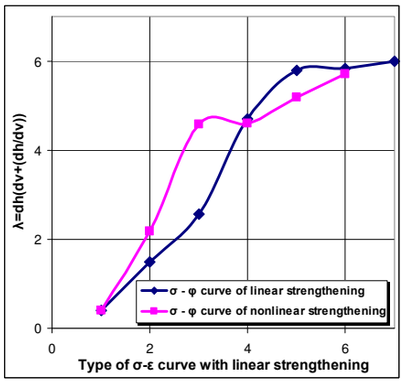

Fig. 13. Dependence of index of outer corner shapes on the type of strengthening curve

3.1.2 Mechanical and structural properties after ECAP

The change of mechanical properties in dependence on number of ECAP passes is shown in Fig. 14. Ultimate tensile strength (UTS) is slightly sensitive on ECAP passes and substructure formation. Yield strength (0,2% YS) is decreasing up to 6th pass where achieved local minimum. From 6th up to 12th pass is growing. Elongation to failure (El.) is inversing to 0,2% YS. Microhardness dependence is given in Fig. 15 from which resulting microhardness growth with an increase of ECAP passes.

TEM analysis was performed on samples after 4th, 6th, 8th and 12th ECAP passes and shown in Fig. 16 - 20.

Initial structure is creating with large polyedric grains (d_g ~ 650 μm) and low dislocation density. Cell substructure with subgrain diameter d_{sg} ~ 2,6 μm was searched after 4th and 6th ECAP passes and are given in Fig. 17, 18. Dislocations are generated with plastic deformation and arranged to dislocation walls, which later transform to subgrains with low or high angles, as it is seeing in Fig. 19. Subgrains are equiaxial with average size d_{sg} ~ 2,2 μm.

Substructure after 12th ECAP pass is equiaxial with low misorientation and average subgrain size d_{sg} ~ 1 μm (Fig. 20). Average subgrain size in dependence to number ECAP passes is given in Fig. 21. The significant substructure refinement was observed after 6th ECAP pass. Yield strength starts to grow also after 6th pass, what coincide with strengthening from grain size refinement after the Hall-Petch equation. Random coarse grains in fine structure matrix were observed after 4th and 12th ECAP pass as shown in Fig. 22.

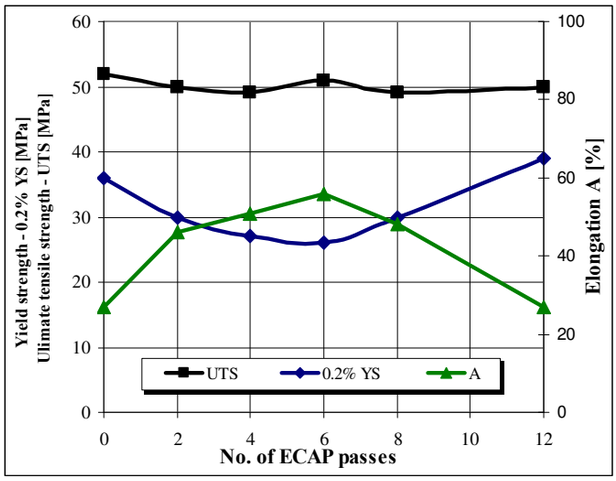

Fig. 14. Development of mechanical properties on ECAP passes

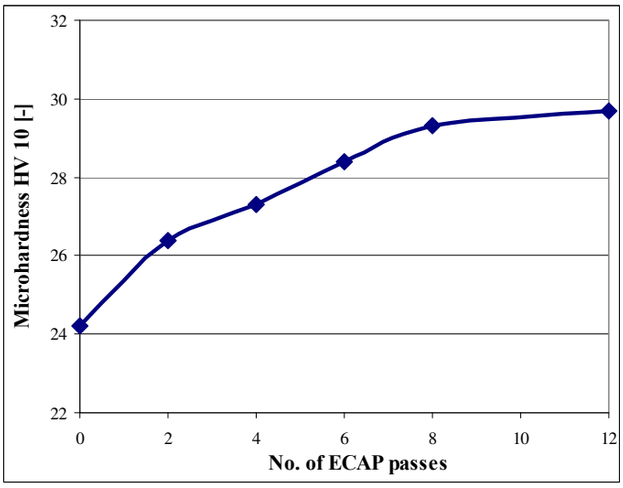

Fig. 15. Microhardness change on ECAP passes

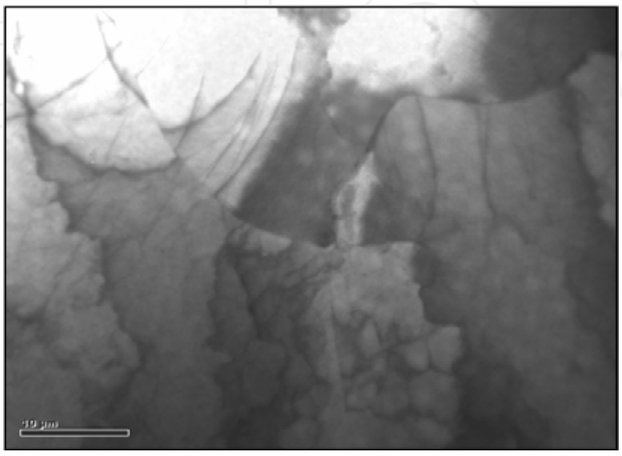

Fig. 16. TEM micrograph before ECAP (d_g ~ 650 μm)

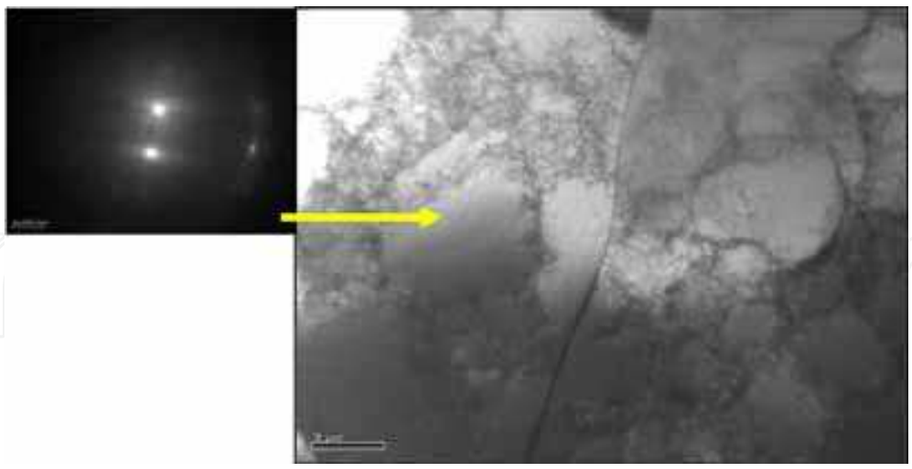

Fig. 17. TEM micrograph after 4th ECAP pass (d_{sg} ~ 2,6 μm)

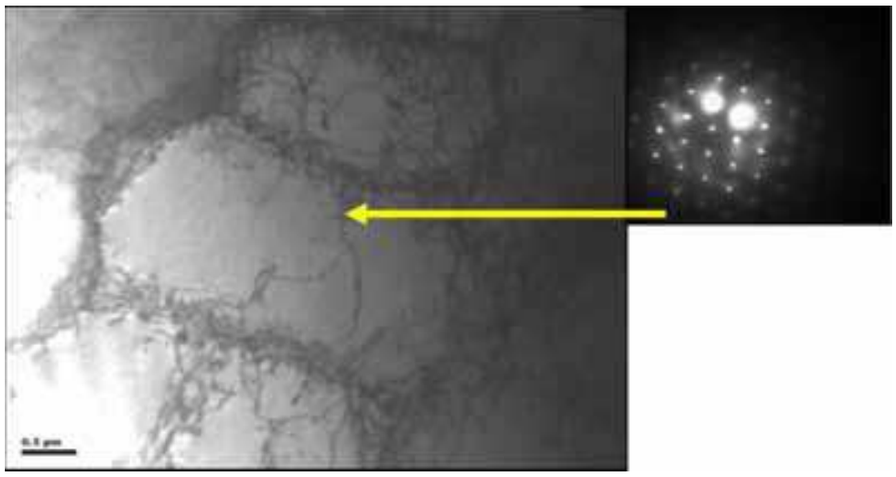

Fig. 18. TEM micrograph after 6th ECAP pass (d_{sg} ~ 2,6 μm)

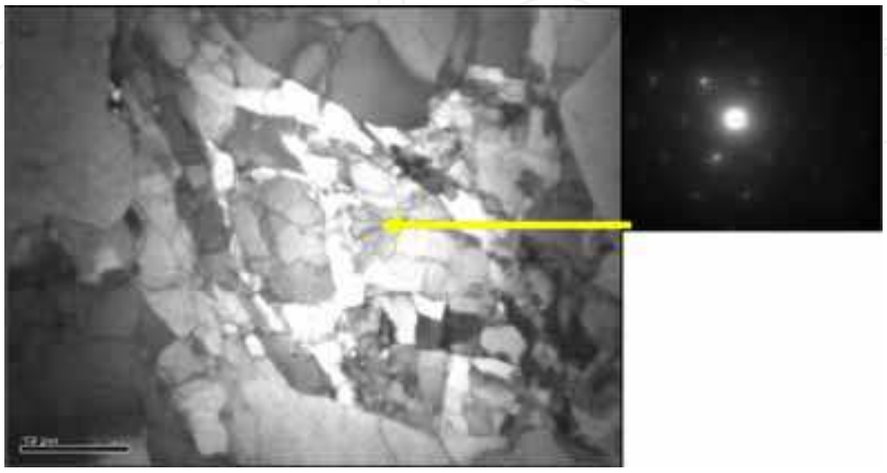

Fig. 19. TEM micrograph after 8th ECAP pass (d_{sg} ~ 2,6 μm)

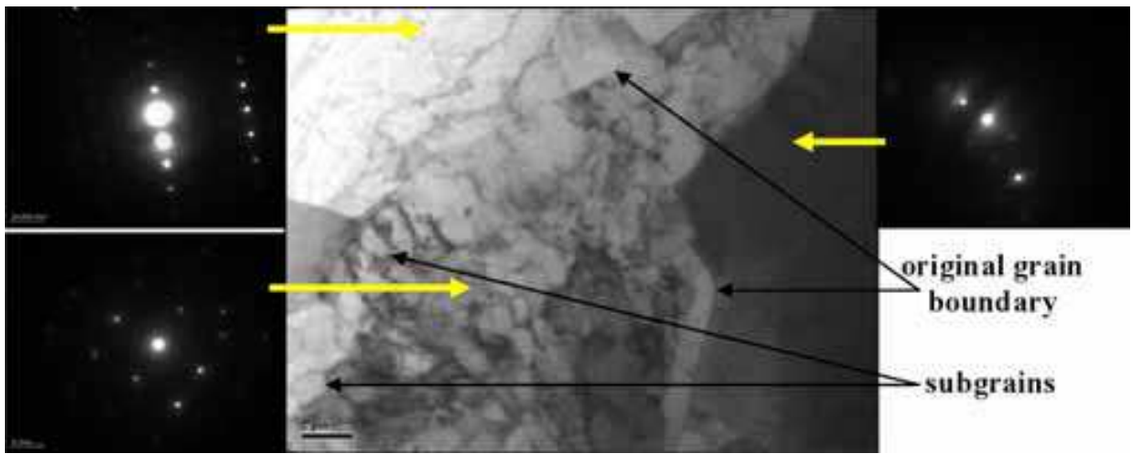

Fig. 20. TEM micrograph after 12th ECAP pass (d_{sg} ~ 0,98 μm)

This anomaly is nucleus of recrystallized subgrain with high angle grain boundary (HAGB). In literature does not exist clear opinion on high purity aluminium recrystallization at room temperature. Dynamic recovery (DR), dynamic recrystallization (DRX), metadynamic recrystallization (MDRX) and static recrystallization (SRX) are possible mechanisms to formation of fine grain structure with SPD at room temperature. Recrystallization of high purity aluminium (99,999%) deformed at room temperature was described (Choi et al., 1994) as DRX and as SRX. Less pure aluminium very slowly recrystallized with comparison of 99,999% pure aluminium (Kim et al., 2003); (Kim et al., 2007). From the literature analysis is resulting intensive sensitivity of aluminium softening (dynamic or static mechanism) in dependence on aluminium purity.

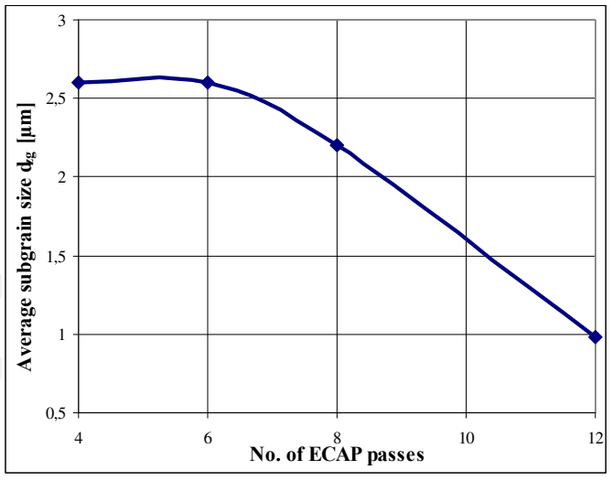

Fig. 21. Grain size change on ECAP passes

The measurement of deformation forces for two material grades (high purity aluminium and oxygen free high conductivity Cu) during ECAP processing were performed by tensometric sensors. The deformation forces were recalculated on deformation stresses and insert to Fig. 23. From graphical dependences are resulting two curve developments. One with decreasing and the other with increasing of deformation stresses. Deformation stress decreasing was observed for aluminium material and increasing for copper material.

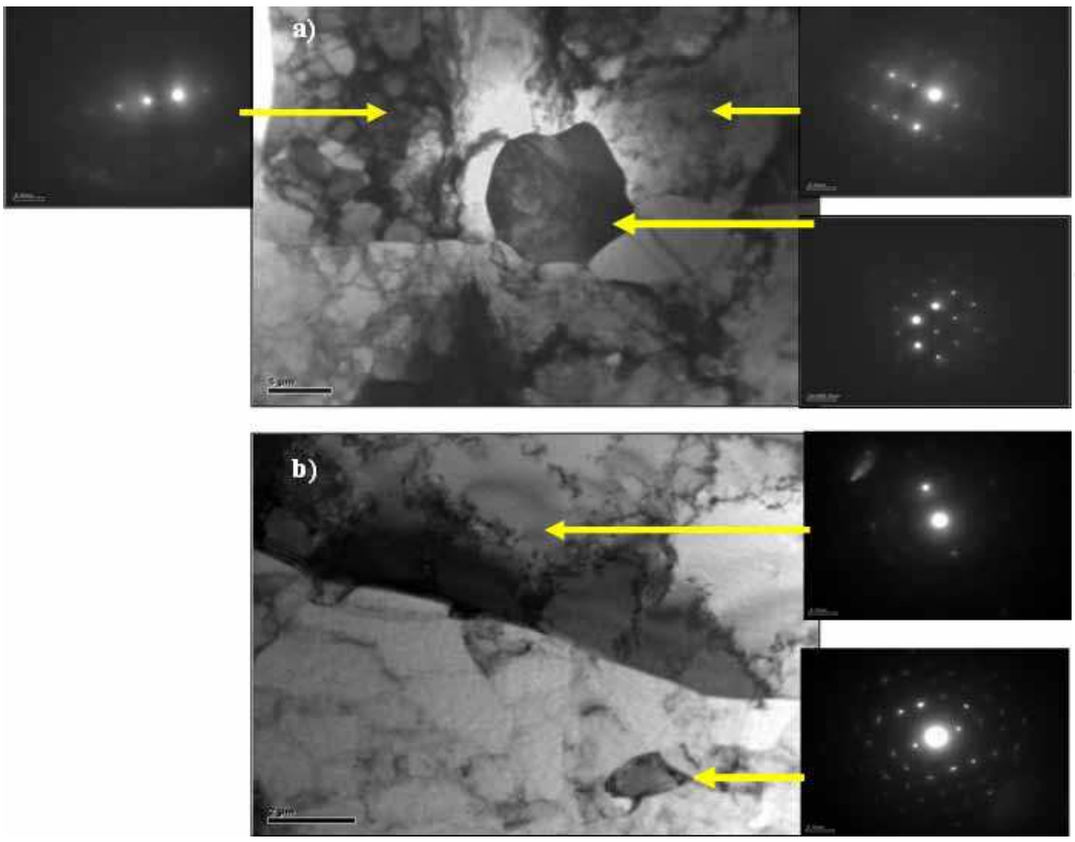

Fig. 22. Recrystallized grains after ECAP processing: a) 4th ECAP pass; b) 12th ECAP pass

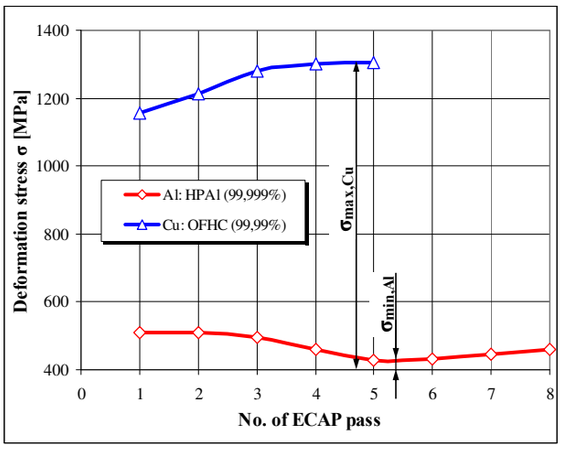

Fig. 23. Dependence of deformation stresses on ECAP passes for different materials

The deformation stress changes with connection of stacking fault energy (SFE) are observed. The high purity aluminium is material with high SFE on level 166 m.J.m^{-2} while OFHC copper is distinguishing with low SFE on level 40 m.J.m^{-2} (Humphreys & Hartherly, 1996); (Neishi et al., 2002).

The materials with high SFE are characterized with dynamic recovery while materials with low SFE by deformation strengthening follow by some kind of recrystallization mechanisms

what have good correlation with observed graphical experimental dependences. Therefore investigated high purity aluminium material is characterized up to 6th ECAP pass with decreasing of deformation stress caused by dynamic recovery and from 6th ECAP pass deformation stress is slightly growing. Similar development of yield strength dependence and inverse dependence of elongation were observed up to 6th and from 6th ECAP passes (Fig. 14). These characteristics dependences from 6th ECAP pass are related on the mechanical strengthening mechanism resulting from refinement of grain size (Fig. 21). On the other side dependence of deformation stress for OFHC copper is growing with the increasing of ECAP passes because of Cu is material with low SFE and mechanical strengthening can be subsequently accompany by some kind of recrystallization process. From Fig. 23 is resulting that ratio between deformation stresses in the 5th ECAP pass ($\sigma_{max,Cu}/\sigma_{min,Al}$) for high purity aluminium and OFHC copper has value 0,33. That means softening mechanisms realized by dynamic recovery was needed only 33% from maximal level of deformation stress occasioning mechanical strengthening which can be subsequently accompanying with possibility of recrystallization process.

3.2 Experimental results and discussion for Al-Cu-Mg-Zr aluminium alloy

3.2.1 Mechanical properties

The stress-strain curves under various processing conditions are plotted in Fig. 24.

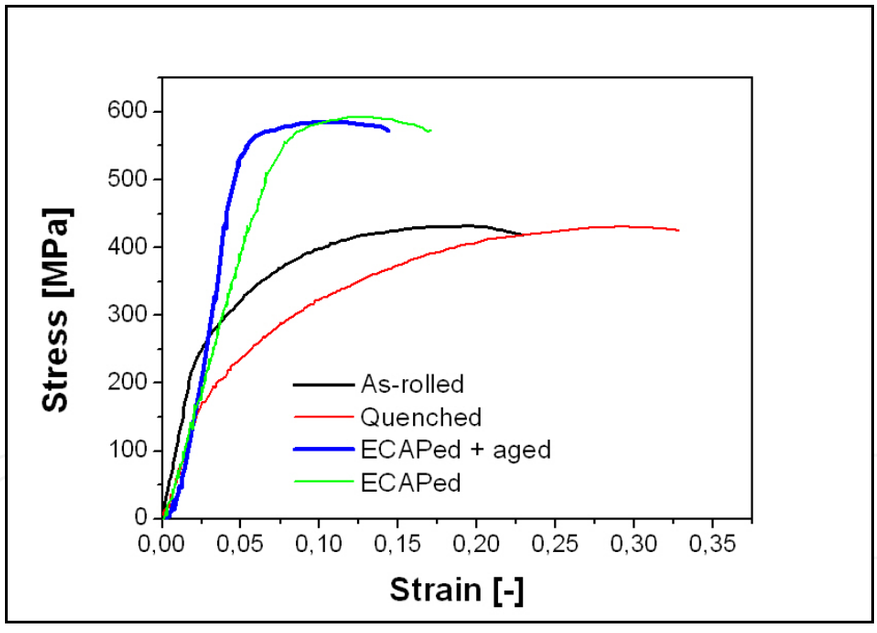

Fig. 24. Stress-strain curves of Al-Cu-Mg-Zr aluminium alloy prepared by different processing conditions

The implementation of SPD via ECAP method caused an increase in materials strength if compared to both systems without application of SPD (as-rolling and quenching). Markedly strengthening of materials after first pass was observed by authors (Vedani et al., 2003); (Cabbibo & Evangelista, 2006); (Kvačkaj et al., 2010). Strengthening of material is caused by grains refinement and strain hardening of solid solution.

The tensile results under various processing conditions are summarized in Table 5.

Processing	Mechanical properties			
	YS [MPa]	UTS [MPa]	El. [%]	Re. [%]
As-rolled	235	381	22,3	27,8
Quenched	157	394	32,8	34,4
ECAPed	511	593	17,1	18,0
ECAPed + aged	515	541	14,4	14,0

Table 5. Mechanical properties of investigated aluminium alloys Al-Cu-Mg-Zr

The difference in the strength values is basically due to the various materials modification. The reason for the increasing of strength and ductility in case of the as-rolled state in comparison to the quenched state was the reduction of strain hardening. The reason for the strength increasing in ECAP was SPD of analyzed alloy, which caused also a sensible decrease of ductility. ECAP increased the strength value approximately 35 % if compared to the as-rolled and quenched alloy. Values of yield strength of approximately 55 % and 70 % separately, of the as-rolled and quenched material were obtained. Overall very good complex mechanical and plastic properties were obtained after ECAP: yield strength of 511 MPa, ultimate tensile strength of 593 MPa, tensile elongation of 17,1 % and reduction in area of 20 %. It is clear that the result of such grains refinement is first of all related to the improvement of mechanical properties; it also increases markedly the density of lattice defects in the solid solution of Al-based alloys and thus accelerates the precipitation process of strengthening particles during the subsequent ageing (Valiev & Langdon, 2006), (Lowe & Valiev, 2000). Finally, present results show that grain refinement by ECAP can lead to a unique combination of strength and ductility. The achieved mechanical properties by ECAP and subsequent treatment can be useful for producing high strength and good ductility in precipitation-hardened alloys.

3.2.2 Fracture and structure investigation

The fracture surfaces analyses of investigated materials showed dominant of transcrystalline ductile fracture. The effect of plastic deformation was revealed in particles cracking for the relevant materials that are typical for aluminium alloys (Nový et al., 2005), (Ovid'ko, 2007); (Nový et al., 2009). During plastic deformation, particles were cracked and/or particles were divided from interphase surface by means of cavity failure systems, which after that exhibited in the formerly dimples, Fig. 25 and Fig. 26.

Detailed fractographical examinations revealed that there were two categories of dimples of transcrystalline ductile fracture: large dimples with average diameter in the range from 5 to 25 μm (arrow in Fig. 27 a), formed by the intermetallic particles on the bases of Fe and Si, which can be to visible by metallography examination (arrow in Fig. 28 b) and small dimples with average diameter in the range from 0,5 to 2,5 μm, formed by submicroscopic and dispersive particles, which were observed by TEM investigation, Fig. 26.

Different average diameters of dimples were obtained for the investigated materials, according to the treatment: as-rolled approximately 10 μm, quenched approximately 9,5 μm, ECAPed approximately 8,5 μm and ECAPed + aged approximately 7,8 μm. The difference between dimples was affected by various processing conditions. For the as-rolled state, the initiator can be identified in the $CuAl_2$ particles, while for the quenched; the role of initiators takes intermetallic particles based of Fe and Si. The SPD via ECAP method caused grains refinement, strain hardening of solid solution and intermetallic deformed particles.

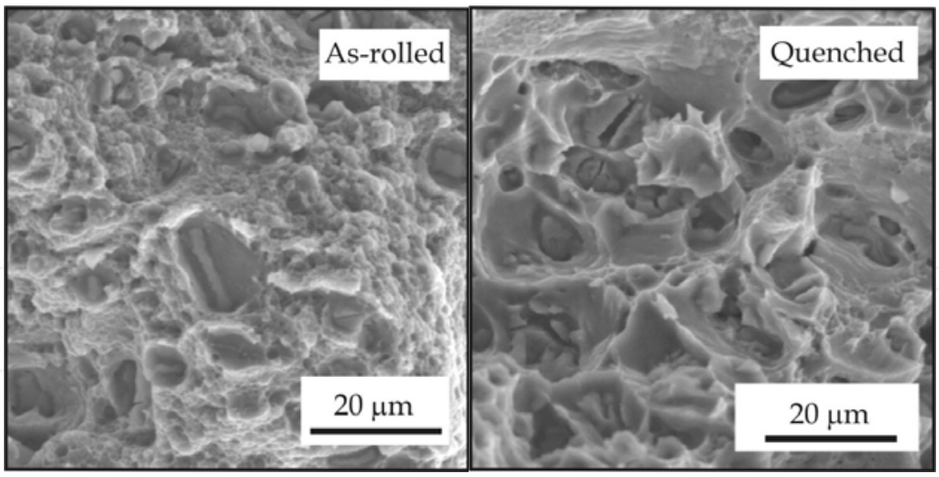

Fig. 25. Transcrystalline ductile fracture as-rolled state and quenched state

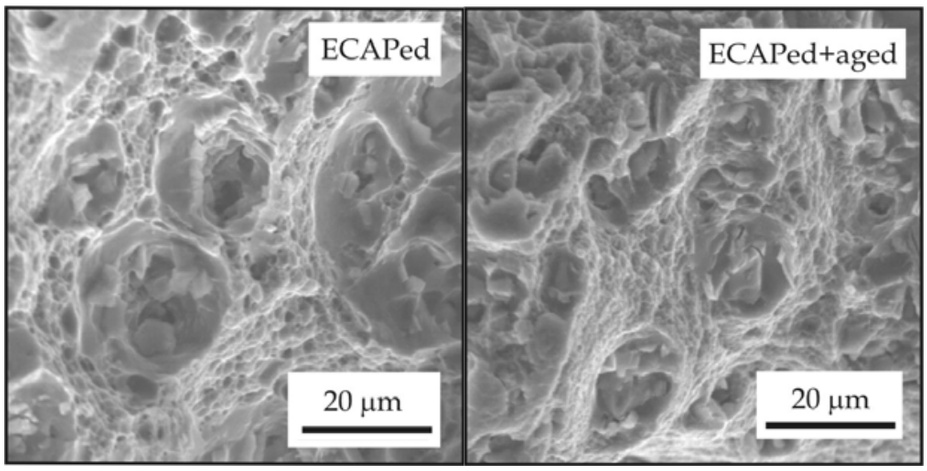

Fig. 26. Transcrystalline ductile fracture ECAPed state, and ECAPed + aged state

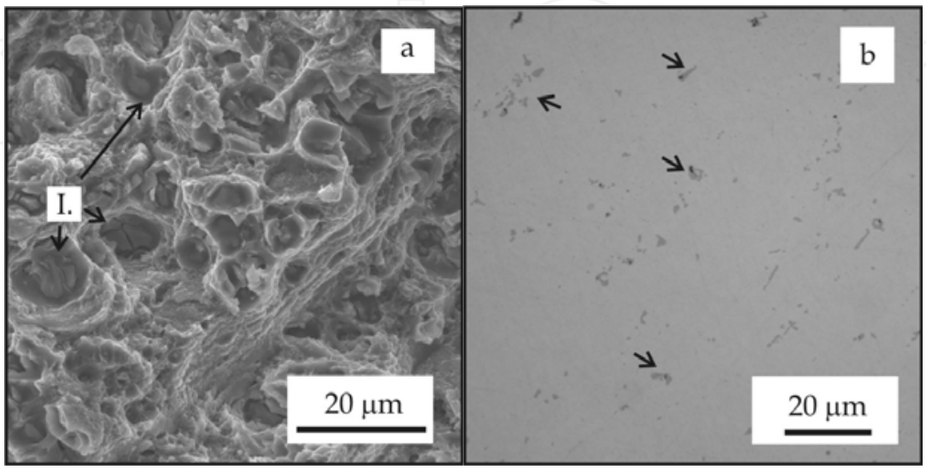

Fig. 27. a, b Intermetallic particles on the base of Fe and Si as a initiators of large dimples

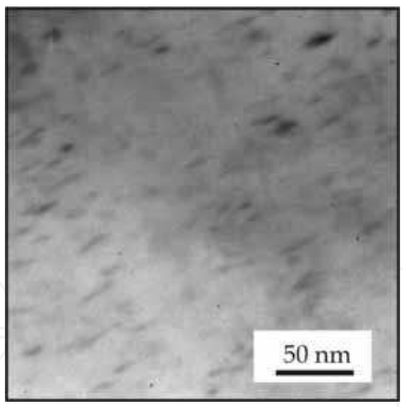

Fig. 28. TEM analyses revealed submicroscopic and dispersive particles as an initiators of small dimples

3.2.3 FEM investigation

Distributions of equivalent plastic deformation after one ECAP pass for both conditions are presented in the Fig. 29.

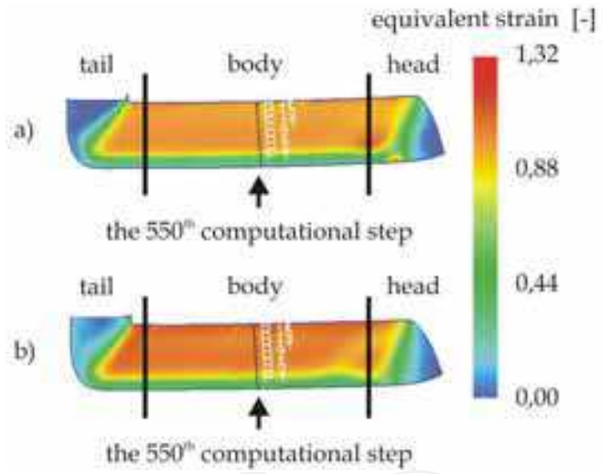

Fig. 29. Distribution of equivalent strain after one ECAP pass at the same forming condition: a) database material, and b) experimental material

Fig. 29 shows, that plastic deformation is non-uniformly distributed along the cross-section and also the length of specimen.

Along the workpiece length is possible to divide the plastic deformation into three deformation areas:

head – non-uniformity of plastic deformation is caused by non-uniformly material flow during junction from vertical to horizontal canal,

body – steady state of plastic deformation,

tail – non-uniformity of plastic deformation is related to the uncompleted pressing of specimen during the exit channel.

Non-uniformity of plastic deformation most be concentrated to the bottom part of the workpiece, in accordance with authors (Kvačkaj et al., 2007); (Kočiško et al., 2009); (Li et al., 2004); (Leo et al., 2007). Due to this fact, the material properties after ECAP are carried out only from body of specimen.

The Fig. 30 illustrates the distribution of equivalent plastic deformation in cross-section part of specimen for the 550th computational step (steady state area of plastic deformation) of both conditions.
Local changes were observed in maximum of curve, where the simulation analysis with database characteristic achieved effective strain value of 1,12 while in simulation analysis with experimental characteristic attained 1,2. The difference represented 7 %. That means the entry data from stress-strain curves did not affect the distribution of plastic deformation intensity in cross-section area of workpiece.

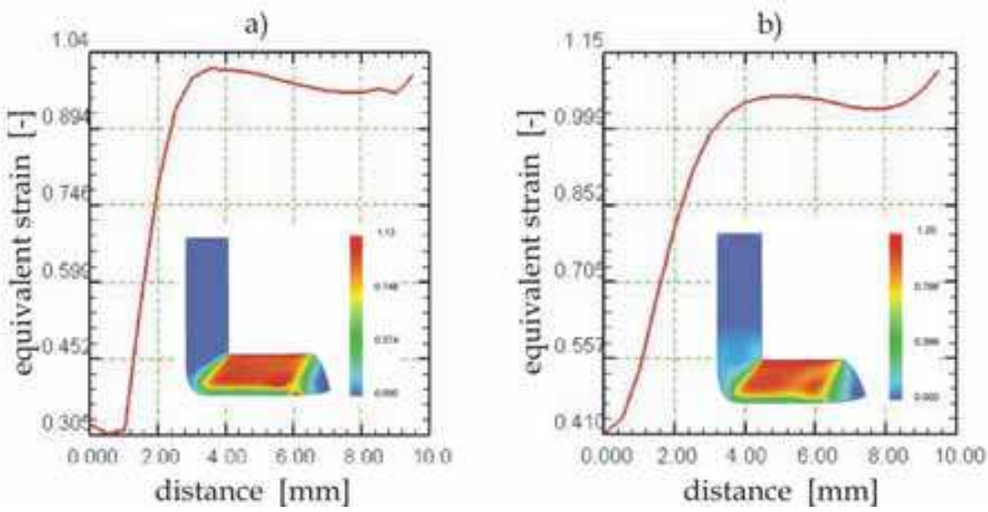

Fig. 30. Distribution of equivalent strain in cross-section part of workpiece in 550th computational step: a) database material, and b) experimental material

Fig. 31 illustrates the distribution of strain rate intensity for both conditions. Strain rate determined the plastic deformation area and/or the plastic deformation zone (PDZ). It can be seen that strain rate is concentrated in the narrow zone – PDZ. In all cases, the plastic deformation zone varies both along the workpiece axis and along the transverse direction from top to bottom as it is confirmed in (Kvačkaj et al., 2007). It is needed to keep in mind that ECAP deformation is generally non-homogeneous, especially when the die is rounded or if conditions lead to a free surface corner gap (Li et al., 2004). However, a disadvantage of the FE studies is that various different combinations like the workpiece, die design, the friction conditions, etc. are applied. All mentioned factors can deeply influence the simulation results and therefore make it difficult to compare results from different studies. Hence, studies for understanding PDZ during the forming process and interpreting the real forming conditions in ECAP process are still lacking.
It can be found from the distribution of strain rate intensity (the 550th computational step in the Fig. 31) that the strain rates are clearly different in case of the database and experimental material; in the inner side of the channel achieved an increase in strain rate about 29 % for experimental material characteristics.
Fig. 32 enables to interpret a temperature development during ECAP process.
Results from Fig. 32 that an increase in temperature during the process, from initial ambient temperature to 35,5 °C for database material and to 46 °C for experimental material. An increase in temperature is connected to heat transformation of plastic deformation part. The temperature of workpiece fail to reach a level of restoration processes for both investigated

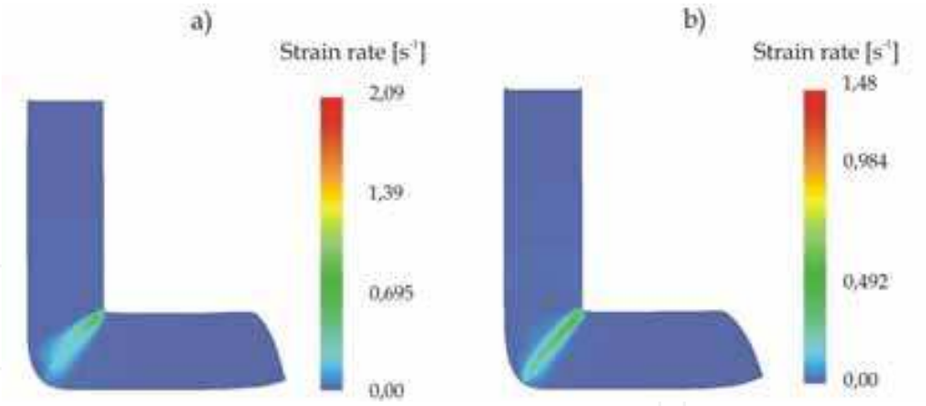

Fig. 31. Distribution of strain rate intensity along to cross-section in 550th computational step: a) database material, and b) experimental material

materials. In simulation to take heat transfer into consideration, for that reason during the ECAP process can to observe a heating of forming tools too. It is important point that temperature of forming tool not allowed to reach a tempering grade. It results from (Kvačkaj et al., 2007) that the significant recovery process can be recognized for temperatures over 300 °C.

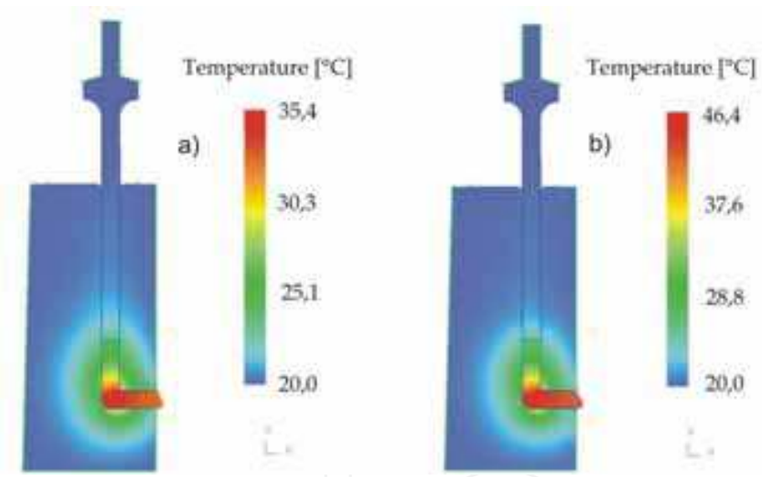

Fig. 32. Temperature development during ECAP process and heating of forming tools: a) database material, and b) experimental material

4. Conclusions

From mathematical simulations of ECAP process by FEM is resulting that the channels filling with material and effective plastic deformations are depends on contact friction, material stress – strain (σ-ε) curves and geometrical definition of ECAP die. Better channels filling by material was observed when friction coefficient was increased. The negligible effect of σ-ε strengthening type curves on channels filling was observed if curves had character rigid – plastic form with linear and nonlinear strengthening. If strengthening curves were approaching to ideal rigid – plastic form with minimal strengthening so differences in channel filling were observed.

The investigation of high purity Al (99,999%Al) material processed by ECAP method refers on slight sensitivity ultimate tensile strength in dependence on ECAP passes. The ultimate

tensile strength was change in interval UTS=49 – 52 MPa. Stronger influence from ECAP passes on yield strength, elongation, microhardness and subgrain diameter was recognized. The values were changed in following intervals: YS=26 – 39 MPa, A=27– 56 %, d_g=650 - 1μm. From the literature analysis is resulting non-uniform opinion on softening mechanisms of high purity Al during or after SPD in ECAP unit. The opinions are recognizing from recovery in dynamic and static regime up to recrystallization in dynamic, metadynamic and static regime. On the essential our results is resulting for high purity Al as material with high stacking fault energy, that softening mechanism up to 6th ECAP pass is dynamic recovery, whereas from 6th ECAP pass the mechanism mechanical strengthening was starting. This supporting viewpoint has good correlation with development of mechanical and substructural properties. On the other side OFHC copper is characterized as material with low stacking fault energy and mechanical strengthening was observed in dependence on ECAP passes. The local dynamic recrystallization grains were observed after 14th ECAP pass. The stress ratio resulting from graphical dependences was $\sigma_{max,Cu}/\sigma_{min,Al}$=0,33, what means that softening mechanisms realized by dynamic recovery needed only 33% from maximal level of deformation stress occasioning mechanical strengthening.

Tensile test results show that, in the stress-strain curves, the stress increased with increasing strain conditions due to severe plastic deformation via ECAP. However, it was observed also that the ECAP exhibited decrease in ductility.

Severe plastic deformation via ECAP may be a very useful process on increasing mechanical properties with only partial decrease and acceptable of ductility. Strengthening of material is caused by grains refinement and strain hardening of solid solution.

Fractographical examinations revealed that there were two categories of dimples of transcrystalline ductile fracture: large dimples, formed by the intermetallic particles and small dimples, formed by submicroscopic and dispersive particles.

The simulation analyses of ECAP process of Al-Cu-Mg-Zr aluminium alloy by means of the commercial two-dimensional finite element code DEFORM shows that in term of prediction individual parameters during forming processing was in the some case (strain rate intensity and temperature) sensible different, providing that material characteristic were given by database or on the basis experimentally determined stress-strain curve. The recorded changes in simulation can be explained to better knowledge of material characteristics from tensile test, by reason that material in them carries the all history of previous technological operations and using a data from program database it needn't exactly to correspond of material selection. In this regard, is necessary to consider in the simulation process to appear from knowledge of material characteristic receives by laboratory test of formability.

5. References

Alexandrov, I. V. , Zhilina, M. V. , Scherbakov, A. V. , Korshunov, A. I. , Nizovtsev, P. N. , Smolyakov, A. A. , Solovyev, V. P. , Beyerlein, I. J. , Valiev, R. Z. (2005). Formation of crystallographic texture during severe plastic deformation. *Archives of Metallurgy and Materials*, Vol. 50, No. 2, (2005) 281-294, ISSN 0860-7052

Balasundar, I. & Raghu, T. (2010). Effect of friction model in numerical analysis of equal channel angular pressing process. *Materials and Design*, Vol. 31, No. 1, (2010) 449-457, ISSN 0261-3069

Beyerlein, I. J. & Tome, C. N. (2004). Analytical modeling of material flow in equal channel angular extrusion (ECAE). *Materials Science and Engineering A*, Vol. 380, No. 1, (2004) 171–190, ISSN 0921-5093

Cabbibo, M. & Evangelista, E. (2006). A TEM study of the combined effect of severe plastic deformation and (Zr), (Sc plus Zr)-containing dispersoids on an Al-Mg-Si alloy. *Journal of Materials Science*, Vol. 41, No. 16, (2006) 5329-5338, ISSN 0022-2461

Cerri, E.; De Marco, P. P. & Leo, P. (2009). FEM and metallurgical analysis of modified 6082 aluminium alloys processed by multipass ECAP: Influence of material properties and different process settings on induced plastic strain. *Journal of Materials Processing Technology*, Vol. 209, No. 3, (2009) 1550-1564, ISSN 0924-0136

Choi, C.; Jeong, J.; Oh, C. & Lee, D. N. (1994). Room temperature recrystallization of 99.999 pct aluminum. *Scripta Metallurgica et Materialia*, Vol. 30, No. 3, (1994) 325-330, ISSN 0956-716X

Chuvil'deev, V. N.; Kopylov, V. I.; Gryaznov, M. Yu.; Sysoev, A. N.; Ovsyannikov B. V. & Flyagin A. A. (2008). Doubling of the strength and plasticity of a commercial aluminum-based alloy (AMg6) processed by equal channel angular pressing. *Doklady Physics*, Vol. 53, No. 11, (2008) 584-587, ISSN 1028-3358

Deform Manual (2003). Scientific Forming Technologies Corporation, version 8.0, Columbus

Dobatkin, S. V.; Zakharov, V. V.; Vinogradov, A. Yu.; Kitagawa, K.; Krasil'nikov, N. A.; Rostova T. D. & Bastarash E. N. (2006). Nanocrystalline structure formation in Al-Mg-Sc alloys during severe plastic deformation. *Russian Metallurgy (Metally)*, Vo. 2006, No 6, (2006) 533-540, ISSN 0036-0295

Dobatkin, S. V. & Sauvage X. (2009). Bulk Nanostructured Multiphase Ferrous and Nonferrous Alloys. In: *Bulk Nanostructured Materials*. Editor(s): Zehetbauer, M. J. & Zhu, Y. T. , 569-603,Wiley-VCH Verlag, ISBN 978-3-52731524-6, Weinheim

Dutkiewicz, J.; Masdeu, F.; Malczewski, P. & Kukuła, A. (2009). Microstructure and properties of α + β brass after ECAP processing. *Archives of Materials Science and Engineering*, Vol. 39, No. 2, (2009) 80-83, ISSN 1897-2764

Han, B. Q.; Lavernia, E. J. & Mohamed, F.A. (2005). Mechanical properties of nanostructured materials. *Reviews on Advanced Materials Science*, Vol. 9, No. 1, (2005) 1-16, ISSN 16065131

Humphreys, F.J. & Hartherly, M. (1995) *Recrystallization and related annealing phenomena*, Pergamon Press, ISBN 13: 9780080418841, Oxford

Figueiredo, R. B.; Pinheiro, I. P.; Aguilar, M. T. P.; Modenesi, P. J. & Cetlin, P. R. (2006). The finite element analysis of equal channel angular pressing (ECAP) considering the strain path dependence of the work hardening of metals. *Journal of Materials Processing Technology*, Vol. 180, No. 1-3, (2006) 30-36, ISSN 0924-0136

Mahallawy, N. E.; Shehata, F. A.; Hameed, M. A. E.; Aal, M. I. A. E. & Kim, H. S. (2010). 3D FEM simulations for the homogeneity of plastic deformation in Al–Cu alloys during ECAP. *Materials Science and Engineering A*, Vol. 527, No. 6, (2010) 1404-1410, ISSN 0921-5093

Maziarz, W.; Dutkiewicz, J.; Lityńska-Dobrzyńska, L.; Santamarta, R. & Cesari, E. (2010). Structure investigations of ferromagnetic Co-Ni-Al alloys obtained by powder metallurgy. *Journal of Microscopy*, Vol. 237, No. 3, (2010) 374-378, ISSN 0022-2720

Medeiros, N.; Lins, J. F. C.; Moreira, L. P. & Gouvêa, J. P. (2008). The role of the friction during the equal channel angular pressing of an IF-steel billet. *Materials Science and Engineering A*, Vol. 489, No. 1-2, (2008) 363-372, ISSN 0921-5093

Meyers, M.A.; Mishra, A. & Benson, D.J. (2006). Mechanical properties of nanocrystalline materials. *Progress in Materials Science*, Vol. 51, No. 4, (2006) 427-556, ISSN 00796425

Michna, Š.; Lukáč I.; et al. (2007). *Aluminium Materials and Technologies from A to Z*, Adin, ISBN 978-80-89244-18-8, Prešov.

Mondolfo, L. F. (1976). *Aluminium Alloys: Structures and Properties*. Butterworth-Heinemann, ISBN 0408706805, Oxford

Neishi, K.; Horita Z. & Langdon, T. G. (2002). Grain refinement of pure nickel using equal-channel angular pressing. *Materials Science and Engineering A*, Vol. 325, No. 1-2, (2002) 54–58, ISSN 0921-5093

Nový, F.; Palček, P. & Chalupová, M. (2005). Failure of Al-alloy AK 4-1c under creep-fatigue interaction conditions. *Kovove Materialy*, Vol. 43, No. 6, (2005) 447-456, ISSN 0023-432X

Nový, F.; Janeček, M. & Král, R. (2009). Microstructure changes in a 2618 alluminium alloy during ageing and creep. *Journal of Alloys and Compounds*, Vol. 487, (2009) 146-151, ISSN 0925-8388

Oh, S.J. & Kang S.B. (2003). Analysis of the billet deformation during equal channel angular pressing; *Materials Science and Engineering A*, Vol. 343, No. 1-2, (2003) 107-115, ISSN 0921-5093

Ovid'ko, I.A. (2005). Superplasticity and ductility of superstrong nanomaterials. *Reviews on Advanced Materials Science*, Vol. 10, No. 2, (2005) 89-104, ISSN 16065131

Ovid'ko, I.A. (2007). Review on the fracture processes in nanocrystalline materials. *Journal of Materials Science*, Vol. 42, No. 5, (2007) 1694-1708, ISSN *0022-2461*

Kim, H. S. (2001). Finite element analysis of equal channel angular pressing using a round corner die. *Materials Science and Engineering A*, Vol. 315, No. 1-2, (2001) 122-128, ISSN 0921-5093

Kim,W. J.; Chung, C. S.; Ma, D. S.; Hong, S. I. & Kim, H. K. Optimization of strength and ductility of 2024 Al by equal channel angular pressing (ECAP) and post-ECAP aging. *Scripta Materialia,*Vol. 49, No. 4, (2003) 333-338, ISSN 1359-6462

Kim, W. J. & Wang, J.Y. (2007). Microstructure of the post-ECAP aging processed 6061 Al alloys. *Materials Science and Engineering A,* Vol. 464, No. 1-2, (2007) 23–27, ISSN 0921-5093

Kobayashi, S.; Oh, S. I. & Altan, T. (1989). *Metal Forming and the Finite-Element Method, 1 ed.*, Oxford University Press, ISBN 978-0-19-504402-7, New York

Kočiško, R.; Kvačkaj, T.; Bidulská, J. & Molnárová, M.: New geometry of ECAP channel. *Acta Metallurgica Slovaca*, Vol. 15, No. 4, (2009) 228-233, ISSN 1335-1532

Kopylov, V. I. & Chuvil'deev, V. N. (2006). The Limit of Grain Refinement during ECAP Deformation. In: Severe Plastic Deformation: Towards Bulk Production of Nanostructured Materials, Burhanettin, S. A. Ed., Nova Science Publishers, 37-58, ISBN 1-59454-508-1, New York

Kováčová, A.; Kvačkaj, T.; Kvačkaj, M.; Pokorný, I.; Bidulská, J.; Tiža J. & Martikán M. (2010). The mechanical properties progress depending on strain rate and load investigation during ecap process. *Acta Metallurgica Slovaca*, Vol. 16, No. 2, (2010) 91-96, ISSN 1335-1532

Kvačkaj, T.; Sokolová, L.; Vlado M.; Vrchovinský V.; Mišičko, R. & Nový, Z. (2004). Influence of pulsation deformations on properties of steel grade Cr18Ni10. *High Temperature Materials and Processes,* Vol. 23, No. 1, (2004) 1-5, ISSN 0334-6455

Kvačkaj, T.; Sokolová, L.; Vlado, M. & Vrchovinský, V. (2005). Influence of deformation temperature and time on the mechanical properties of pulsation deformed stainless steel. *High Temperature Materials and Processes,* Vol. 24, No. 2, (2005) 139-144, ISSN 0334-6455

Kvačkaj, T.; Zemko, M.; Kočiško, R.; Kuskulič, T.; Pokorný, I.; Besterci, M.; Sülleiová, K.; Molnárová, M. & Kováčová, A. (2007). Simulation of ECAP process by finite element method. *Kovove Materialy*, Vol. 45, No. 5, (2007) 249-254, ISSN 0023-432X

Kvačkaj, T.; Kováčová, A.; Kvačkaj, M.; Pokorný, I.; Kočiško, R. & Donič, T. (2010). Influence of strain rate on ultimate tensile stress of coarse-grained and ultrafine-grained copper. *Materials Letters*, Vol. 64, No. 21, (2010 a) 2344-2346, ISSN 0167-577X

Kvačkaj, T.; Bidulská, J.; Fujda, M.; Kočiško, R.; Pokorný, I. & Milkovič, O. (2010). Nanostructure formation and properties in some Al alloys after SPD and heat treatment. *Materials Science Forum*, Vol. 633-634, (2010 b) 273-302, ISSN 0255-5476

Li, S.; Bourke, M. A. M.; Beyerlein, I. J.; Alexander, D. J. & Clausen B. (2004). Finite element analysis of the plastic deformation zone and working load in equal channel angular extrusion. *Materials Science and Engineering A*, Vol. 382, No. 1-2, (2004) 217-236, ISSN 0921-5093

Lityńska-Dobrzyńska, L.; Dutkiewicz, J.; Maziarz, W. & Rogal, ł. (2010). TEM and HRTEM studies of ball milled 6061 aluminium alloy powder with Zr addition. *Journal of Microscopy*, Vol. 237, No. 3, (2010) 506-510, ISSN 0022-2720

Lowe, T. C. & Valiev, R. Z. (2000). *Investigations and Applications of Severe Plastic Deformation,* Kluwer Academic Publishers, ISBN 0-7923-6280-2, Dordrecht, Netherlands

Leo, P.; Cerri, E.; De Marco, P. P. & Roven H. J. (2007). Properties and deformation behaviour of severe plastic deformed aluminium alloys. *Journal of Materials Processing Technology*, Vol. 182, No. 1-3 (2007) 207-214, ISSN 0924-0136

Pernis, R.; Kasala, J. & Bořuta J. (2009). Hot torsion tests of cartridge brass MS70. *Acta Metallurgica Slovaca*, Vol. 15, No. 1, (2009) 5-14, ISSN 1335-1532

Semiatin, S. L.; Delo, D. P. & Shell, E. B. (2000). The effect of material properties and tooling design on deformation and fracture during equal channel angular extrusion. *Acta Materialia*, Vol. 48, No. 8, (2000) 1841-1851, ISSN 1359-6454

Stoica, G.M.; Fielden, D.E.; McDaniels, R.; Liu, Y.; Huang, B.; Liaw, P.K.; Xu, C. & Langdon, T.G. (2005). An analysis of the shear zone for metals deformed by equal-channel angular processing. *Materials Science and Engineering A*, Vol. 410–411, (2005) 239–242, ISSN 0921-5093

Valiev, R. Z.; Islamgaliev, R. K. & Alexandrov I. V. (2000). Bulk nanostructured materials from severe plastic deformation. *Progress in Materials Science,* Vol. 45, No. 2, (2000) 103-189, ISSN 0079-6425

Valiev, R. Z. & Langdon, T. G. (2006). Principles of equal-channel angular pressing as a processing tool for grain refinement. *Progress in Materials Science,* Vol. 51, No. 7, (2006) 881-981, ISSN 0079-6425

Vedani, M.; Bassani, P.; Cabibbo, M. & Evangelista, E. (2003). Experimental aspects related to equal channel angular pressing of a commercial AA6082 alloy. *Metallurgical Science and Technology*, Vol. 21, No. 2, (2003) 3-9, ISSN 0393-6074

Yoon, S. Ch. & Kim, H. S. (2008). Finite element analysis of the effect of the inner corner angle in equal channel angular pressing. *Materials Science and Engineering A*, Vol. 490, No. 1-2, (2008) 438-444, ISSN 0921-5093

Zhernakov, V. S., Budilov, I. N., Raab, G. I., Alexandrov, I. V. & Valiev, R. Z. (2001). A numerical modelling and investigations of flow stress and grain refinement during equal-channel angular pressing. *Scripta Materialia*, Vol. 44, No. 8-9, (2001) 1765-1769, ISSN 1359-6462

Zehetbauer, M. J.; Zeipper L. & Schafler E. (2006). Modelling Mechanical Properties of SPD Materials During and After Severe Plastic Deformation. In: *Nanostructured Materials by High-Pressure Severe Plastic Deformation*, NATO Science Series II: Mathematics, Physics and Chemistry, Vol. 212, Zhu, Y. T & Varyukhin, V., 217-226, DOI: 10.1007/1-4020-3923-9_30

Zehetbauer, M. J. & Estrin, Y. (2009). Modeling of Strength and Strain Hardening of Bulk Nanostructured Materials. In: *Bulk Nanostructured Materials*, Zehetbauer, M. J. & Zhu, Y. T. , 109-136,Wiley-VCH Verlag, ISBN 978-3-52731524-6, Weinheim

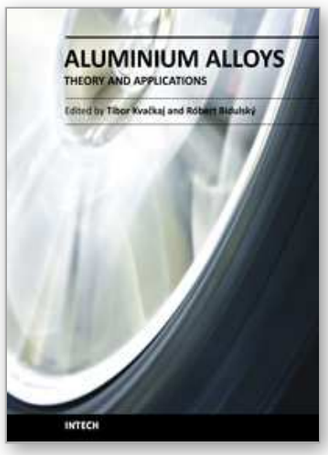

Aluminium Alloys, Theory and Applications

Edited by Prof. Tibor Kvackaj

ISBN 978-953-307-244-9
Hard cover, 400 pages
Publisher InTech
Published online 04, February, 2011
Published in print edition February, 2011

The present book enhances in detail the scope and objective of various developmental activities of the aluminium alloys. A lot of research on aluminium alloys has been performed. Currently, the research efforts are connected to the relatively new methods and processes. We hope that people new to the aluminium alloys investigation will find this book to be of assistance for the industry and university fields enabling them to keep up-to-date with the latest developments in aluminium alloys research.

How to reference

In order to correctly reference this scholarly work, feel free to copy and paste the following:

Tibor Kvačkaj, Jana Bidulská, Robert Kočiško and Róbert Bidulský (2011). Effect of Severe Plastic Deformation on the Properties and Structural Developments of high purity Al and Al-Cu-Mg-Zr Aluminium Alloy, Aluminium Alloys, Theory and Applications, Prof. Tibor Kvackaj (Ed.), ISBN: 978-953-307-244-9, InTech, Available from: http://www.intechopen.com/books/aluminium-alloys-theory-and-applications/effect-of-severe-plastic-deformation-on-the-properties-and-structural-developments-of-high-purity-al

INTECH
open science | open minds

InTech Europe
University Campus STeP Ri
Slavka Krautzeka 83/A
51000 Rijeka, Croatia
Phone: +385 (51) 770 447
Fax: +385 (51) 686 166
www.intechopen.com

InTech China
Unit 405, Office Block, Hotel Equatorial Shanghai
No.65, Yan An Road (West), Shanghai, 200040, China
中国上海市延安西路65号上海国际贵都大饭店办公楼405单元
Phone: +86-21-62489820
Fax: +86-21-62489821

IntechOpen